Comparative analysis of evapotranspiration using the SEBAL model and the evaporimeter pan method in the Huancane basin of Puno, Peru

Aroni-Quispe, Danny, Alfaro-Alejo, Roberto, Huaman-Gutierrez, Hector, Belizario-Quispe, Germán

Danny X. Aroni-Quispe, Roberto Alfaro-Alejo, Hector A. Huaman-Gutierrez, Germán Belizario-Quispe, "Comparative analysis of evapotranspiration using the SEBAL model and the evaporimeter pan method in the Huancane basin of Puno, Peru," Proc. SPIE 11856, Remote Sensing for Agriculture, Ecosystems, and Hydrology XXIII, 118560H (12 September 2021); doi: 10.1117/12.2600821

SPIE.

Event: SPIE Remote Sensing, 2021, Online Only

Comparative analysis of evapotranspiration using the SEBAL model and the evaporimeter pan method in the Huancane basin of Puno, Peru

Danny X. Aroni-Quispe[a], Roberto Alfaro-Alejo*[a], Hector A. Huaman-Gutierrez[a], Germán Belizario-Quispe[a]

[a]Faculty of Agricultural Engineering, National University of Altiplano, Puno, Peru

ABSTRACT

Remote sensing methods allow obtaining important information from the Earth's surface to effectively evaluate agricultural processes. This research work proposes to carry out the comparative analysis of evapotranspiration using the methodologies of the SEBAL model and the evaporimeter pan in the Huancané basin, Peru. The specific objectives were to estimate the evapotranspiration through the SEBAL model from Landsat 8 images, to estimate the real evapotranspiration through the evaporimeter pan method from meteorological data from the Huancané and Muñani stations, for the comparison and validation of the evapotranspiration results obtained. with the SEBAL model. The methodological stages considered are: the collection of meteorological data from the National Meteorology and Hydrology Service (SENAMHI) of Peru and Landsat 8 satellite images, the application of the SEBAL algorithm and the evaporimeter pan method, to obtain evapotranspiration. For the SEBAL model, the lowest evapotranspiration values correspond to areas with soils without crops or with low vegetation cover (NDVI < 0.21) and for areas covered with vegetation or grasslands (NDVI > 0.41) obtaining values between 1.50 to 4.20 mm/day. The evaporimeter pan method allowed to determine the real evapotranspiration (ETR), for the points of location of the weather stations, values that vary between 1.76 to 2.44 mm/day. The comparison and validation of the evapotranspiration values observed (ETR evaporimeter pan) and estimated (ETR SEBAL), for the analysis areas near the Huancane station present a mean square error of 0.26 and 0.25, coefficient of determination of 0.97 and a Nash-Sutcliffe efficiency of 0.81 and 0.83. Likewise, for the areas near the Muñani station where they show a mean square error of 0.13 and 0.14, coefficient of determination of 0.97 and 0.93; and a Nash-Sutcliffe efficiency of 0.81 and 0.82. The results obtained with the SEBAL model are satisfactory, which shows that its use is feasible.

Keywords: Evapotranspiration, Landsat image, SEBAL, Remote sensing, Surface energy balance

1. INTRODUCTION

Evapotranspiration (ET) is important in the interaction between soil, vegetation and the atmosphere, it is a factor in the quantitative evaluation of the energy balance, since many processes and parameters of the environment are influenced, such as the moisture content in the soil, vegetation productivity, nutrient absorption, water balance, among others, particularly in arid and semi-arid areas where water availability is more critical[1,2].

Evapotranspiration occurs due to two phenomena that occurs in the crop-soil relationship, crop transpiration and soil evaporation, it constitutes the fundamental loss of water, from which the need for water of the crops is calculated[3]. Evapotranspiration is a parameter of common interest in climatological, hydrological, agricultural and forestry studies[4]. At present, the proper management and management of water resources is of great importance, due to the increase in the various demands even more in agricultural areas[5,6]. Balances are made between availability and demand, for which evapotranspiration is an input data in the various hydrological models and a parameter obtained from measurements in the field, either with meteorological stations or lysimeters, however, these methods are limited, since they provide point values of evapotranspiration for a specific place and do not provide evapotranspiration on a larger scale[7].

Remote sensing techniques and geographic information systems (GIS) are very useful since they allow us to make spatial estimates, expressed in pixels and in large areas[8].

*ralfaro@unap.edu.pe; phone 51 051366192; fax 51 051366192; www.unap.edu.pe

Remote Sensing for Agriculture, Ecosystems, and Hydrology XXIII, edited by C. M. U. Neale, A. Maltese, Proc. of SPIE Vol. 11856, 118560H · © 2021 SPIE · CCC code: 0277-786X/21/$21 · doi: 10.1117/12.2600821

The proposed model is based on the energy conservation equation and allows the estimation of evapotranspiration using spatial information from different sensors that provide images where visible, infrared, near infrared and thermal radiation are recorded. The great advantage of this method is the greatly reduced data collection in the field and the good results in the evapotranspiration estimates, thanks to the fact that the model includes multiple variables that are responsible for the ET process. This model is called SEBAL[9] (Surface Energy Balance Algorithm For Land). It was used in different fields as the determination of evapotranspiration in different types of crops[10–13], also for evaporation from lakes[14], in different parts of the world.

The present research compares the actual evapotranspiration estimated by the SEBAL model and the evaporimeter pan method, in order to evaluate the efficiency of the SEBAL method. To later apply the SEBAL method to the entire Huancane basin area.

2. MATERIALS AND METHODS

2.1 Study area

The research was carried out in the Huancané basin, Puno region, Peru, geographically comprised between coordinates 14° 31' 26" - 15° 23' 07" south latitude and 70° 07' 06" - 69° 29' 12" longitude west, with an altitude between 3806 and 5100 meters above sea level, which corresponds hydrographically to the hydrographic region of Lake Titicaca. It has an area of 3,631.19 km2 and a length of the main channel of 142 km.

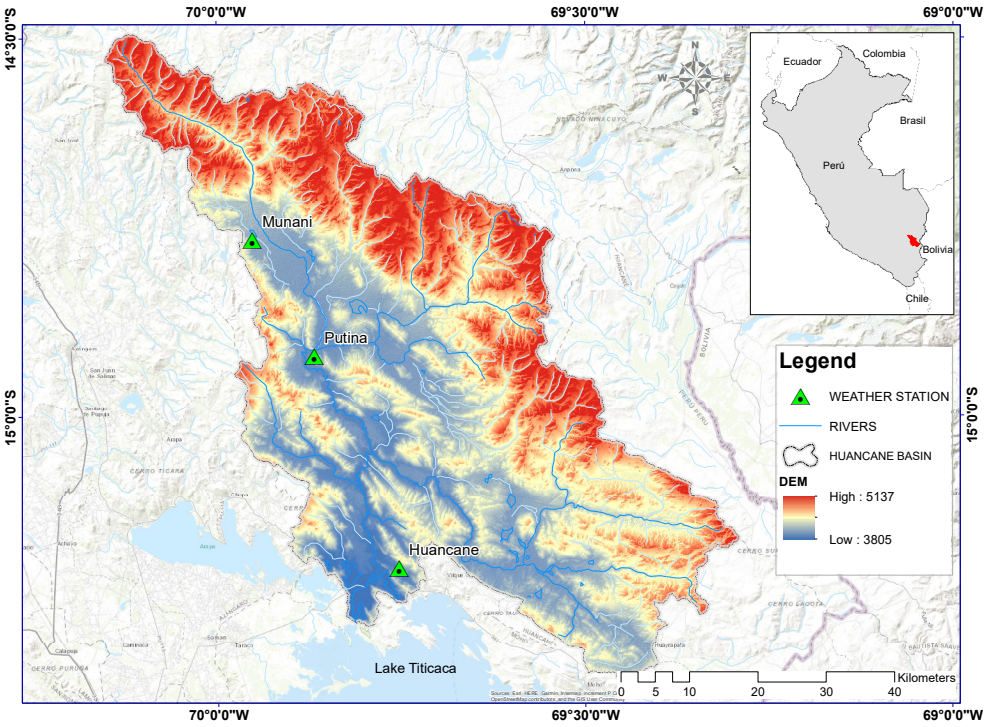

Figure 1. Location of the Huancané basin and weather stations in the basin.

2.2 Materials

Satellite images of the Landsat 8 satellite were used, acquired by the OLI and TIR sensors, managed by the National Space and Space Administration (NASA) and the production - distribution of the images depends on the United States Geological Survey (USGS). The Landsat 8 images have been selected without cloudiness or other errors, they are presented in table 1. Data from two meteorological stations obtained from the database of the National Meteorology and Hydrology Service (SENAMHI) - Peru were also used; the records correspond to daily data of relative humidity in (%), wind speed in (m/s) and evaporation of the class A pan in (mm).

Table 1. Satellite imagery acquisition dates for the study.

No.	Date	Satellite	ID Image	Path/Row	Julian Day
1	26/04/2013	LANDSAT 8	LC80020702013116LGN02	2/70	116
2	29/06/2013	LANDSAT 8	LC80020702013180LGN01	2/70	180
3	31/07/2013	LANDSAT 8	LC80020702013212LGN01	2/70	212
4	16/08/2013	LANDSAT 8	LC80020702013228LGN01	2/70	228
5	03/08/2014	LANDSAT 8	LC80020702014215LGN01	2/70	215
6	07/11/2014	LANDSAT 8	LC80020702014311LGN01	2/70	311
7	06/08/2015	LANDSAT 8	LC80020702015218LGN01	2/70	218
8	20/05/2016	LANDSAT 8	LC80020702016141LGN01	2/70	141
9	23/07/2016	LANDSAT 8	LC80020702016205LGN02	2/70	205
10	26/07/2017	LANDSAT 8	LC80020702017207LGN00	2/70	207
11	11/08/2017	LANDSAT 8	LC80020702017223LGN00	2/70	223
12	29/07/2018	LANDSAT 8	LC80020702018210LGN00	2/70	210

2.3 SEBAL model

The algorithm for Surface Energy Balance (SEBAL), developed by Bastiaanssen, in 1995[9], is a method that allows calculating evapotranspiration using satellite images that record visible, near infrared and thermal radiation, this method is mainly based on the calculation of the variables that make up the energy balance through processes applied to satellite images, greatly reducing data collection in the field[16].

$$\lambda ET = R_n - G - H \tag{1}$$

Equation (1) is the surface energy balance where: λET is the latent heat flux (W/m2), Rn is the net surface radiation flux (W/m2), G is the soil heat flux (W/m2), and H is the sensible heat flux to the air (W/m2).

The net radiation flux (Rn) at the surface represents the radiation energy available at the surface. This is calculated by the difference between the outgoing radiation fluxes and the incoming radiation flux. This can be seen in figure 2 of the radiation balance at the Earth's surface[10,17], is estimated using equation (2).

$$R_n = (1-\alpha)RS\downarrow + RL\downarrow - RL\uparrow - (1-\varepsilon_0)RL\downarrow \tag{2}$$

In equation (2), the amount of shortwave radiation (RS↓) that remains available at the surface is a function of the surface albedo (α). Albedo of the surface is a reflection coefficient, it is defined as the ratio of the reflected radiant flux to the incident radiant flux on the solar spectrum. It is determined using the information of each band of the satellite images, except the thermal bands.

Incoming shortwave radiation (RS↓) is defined using the solar constant, the solar incidence angle, a relative Earth-Sun distance, and a calculated atmospheric transmissivity. Incoming long wave radiation (RL↓) is estimated using the modified Stefan-Boltzmann equation with atmospheric transmissivity and a selected surface reference temperature. Outgoing long wave radiation (RL↑) is calculated using the Stefan-Boltzmann equation with an emissivity (ε_o) of the surface and the estimated surface temperature. Surface temperatures are determined from information contained in the thermal bands of satellite images[18,19].

The magnitude of the flux of heat stored or released by the soil is relatively small in relation to the rest of the fluxes. When a daily time cycle is considered, given a heating and cooling process, its contribution to the energy balance is not considered. If you consider hourly intervals or other than a full day, your contribution may be significant, and they should be included[20].

The flux of heat to the ground is dominated by the energy received at the earth's surface, the capacity and thermal conductivity of the ground. In general, the soil stores heat during the day, in this way there is a storage of energy and at the same time there is a flux of heat towards deeper layers of the soil. At night the process is reversed, that is, the soil

releases the stored energy into the atmosphere, and through a heat gradient there is a flux of energy from the deep layers of the soil[21,22].

In the application of SEBAL to obtain G (equation 1), it depends on the net radiation (R_n), the Normalized Difference Vegetation Index (NDVI), the surface temperature (T_S) and the albedo (α)[18].

$$G = \left(\frac{T_s}{\alpha} (0.0038 \times \alpha^2)(1 - 0.98 \times NDVT^4) \right) \times R_n \quad (3)$$

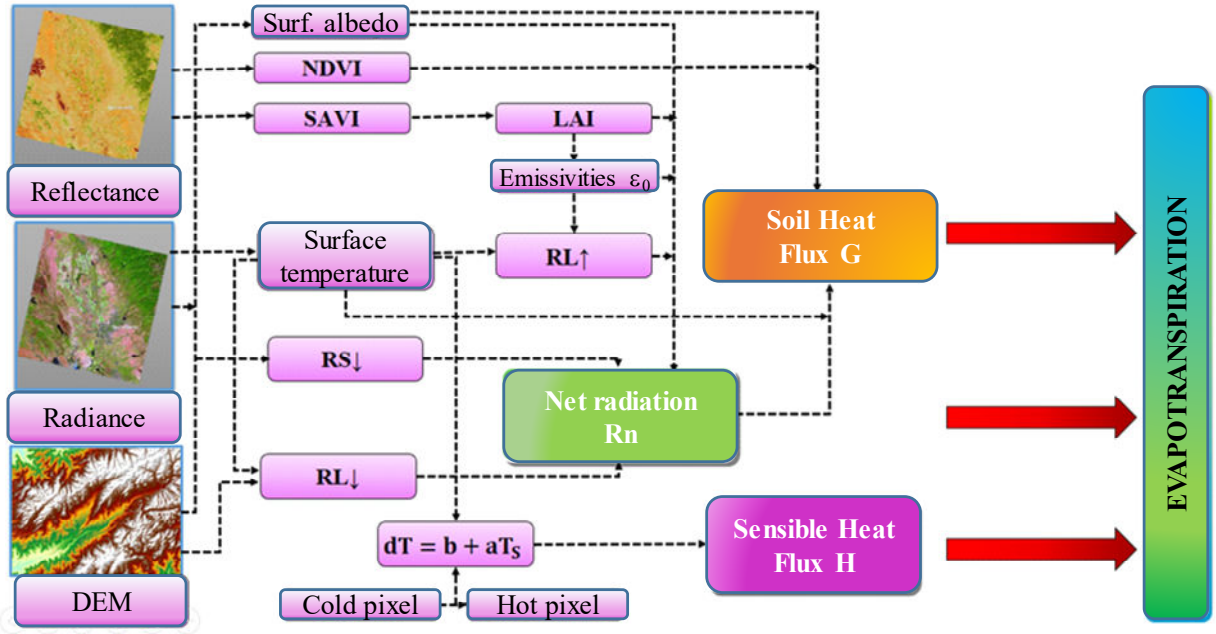

Figure 2. General Methodology flowchart.

The sensible heat flux (H) is the transfer of heat between the soil and the atmosphere, by forced or free convection. H is the heat exchange through air as a result of a temperature gradient between the surface and the atmosphere[23]. The temperature of the earth's surface is higher than the temperature of the air during the day and the sensible heat flux is normally directed upwards. During the night, the situation can be reversed[24].

$$H = \frac{\rho \times C_p (T_s - T_a)}{r_{ah}} \quad (4)$$

Where; ρ is the density of air (kg/m3), C_p is the specific heat of air (1,004J/ kg/K), (T_s-T_a) temperature gradient between the surface and the reference height and r_{ah} is the aerodynamic resistance to heat transport (s/m).

2.4 Hourly evapotranspiration (ET_h)

To obtain the daily evapotranspiration, initially the hourly evapotranspiration is obtained, which is equal to the quotient between the latent heat flux and the latent heat of vaporization ($ETinst = \lambda ET/\lambda$), as indicated in equation (5)[25].

$$ET_h = 3600 \times \frac{\lambda ET}{\lambda} \quad (5)$$

Where: ET_h: Hourly evapotranspiration, expressed in mm/h; λET: Latent heat flux (W/m2), which was calculated with equation (1); λ: Latent heat of vaporization, expressed in J/kg.

Latent heat of vaporization is defined as the amount of energy required to vaporize a unit of mass of water and its estimate depends on the surface temperature, as indicated by equation (6), for example, at 20° C, λ has a value of about 2.45×10^6 J/kg.

$$\lambda = (2.501 - 0.00236 \times (T_s - 273.15)) \times 10^6 \quad (6)$$

Where: T_S: Surface temperature, expressed in K.

2.5 Evapotranspiration fraction

The fraction of evapotranspiration represents the percentage of energy that evaporates, with respect to the energy available to evaporate, and is represented in equation (7).

$$\Lambda = \frac{\lambda ET}{R_n - G} \quad (7)$$

Where: Λ: Evaporative fraction, dimensionless; R_n and G are instantaneous values obtained from the image.

2.6 Daily evapotranspiration (ET_{24})

Daily evapotranspiration values are often more useful than instantaneous evapotranspiration values. The SEBAL model estimates this parameter assuming that the evaporative fraction remains constant 24 hours a day, using equation (8).

$$ET_{24} = \frac{\Lambda \times R_{nd}}{\lambda} \times 86400 \quad (8)$$

Where: ET_{24}: Daily evapotranspiration, expressed in mm/day; Λ: Evaporative fraction, dimensionless; λ: Latent heat of vaporization, expressed in J/kg; 86400: It is the number of seconds in a 24 hour period; R_{nd}: Daily net radiation, expressed in W/m2, is expressed as a function of extraterrestrial daily radiation. The SEBAL model contains an independent model for the calculation of this variable, through equation (9).

$$R_{nd} = (1 - \alpha) \times Ra_{24} \times \tau_{sw} + 110 \times \tau_{sw} \quad (9)$$

Where: α: surface albedo, dimensionless; Ra_{24}: Extraterrestrial daily radiation; τ_{sw}: Atmospheric transmissivity.

Evapotranspiration values were obtained from the evaporimeter pan, using equation (10).

$$ETR = K_C \times ET_0 \quad (10)$$

Where: ETR is the evapotranspiration of the crop, mm; Kc is the dimensionless crop coefficient; and ET_o is the reference evapotranspiration, mm.

The ET_o was the ET obtained by means of an evaporimeter pan in the areas cultivated with grass, adjacent to the meteorological stations; This ET_o was compared with that obtained by Equation (8).

2.7 Field data

Plots (agricultural areas) adjacent and close to the Huancané and Muñani stations of the National Meteorology and Hydrology Service (SENAMHI) were identified; These zones were chosen because they had the necessary meteorological information to estimate the reference evapotranspiration, using the class A evaporimeter pan and later estimate the real evapotranspiration with the Kc values.

The values of crop coefficients Kc considered in official hydrological studies in the Huancané and Suches basins have been used[15], information provided by the Local Administration of Water Huancané (ALA), these values were predicted for the different phases of the vegetative period of the crops.

3. RESULTS

3.1 ET estimation using the SEBAL model

Net radiation (Rn)

In Figure 3 the values of net radiation are shown, for the dates of analysis, these values obtained oscillate between 29.34 and 863.37 W/m2. The variability of Rn results is mainly affected by emissivity and surface albedo. In areas with vegetation they present values between 483.40 to 704.67 W/m2 and in areas without vegetation they present values lower than 483.40 W/m2.

Huaman[26], in his research, he presented net radiation values in areas with vegetation that fluctuate between 400 and 579.4 W/m2 and in desert areas without vegetation, values less than 400 W/m2. Other authors reported values between 400 and 800 W/m2 where the high values correspond to grasslands and the lowest values were presented in areas with bare soils[27]. Therefore, the values obtained in the study agree with the expected values. These values correspond to instantaneous values recorded for the time of passage of the satellite.

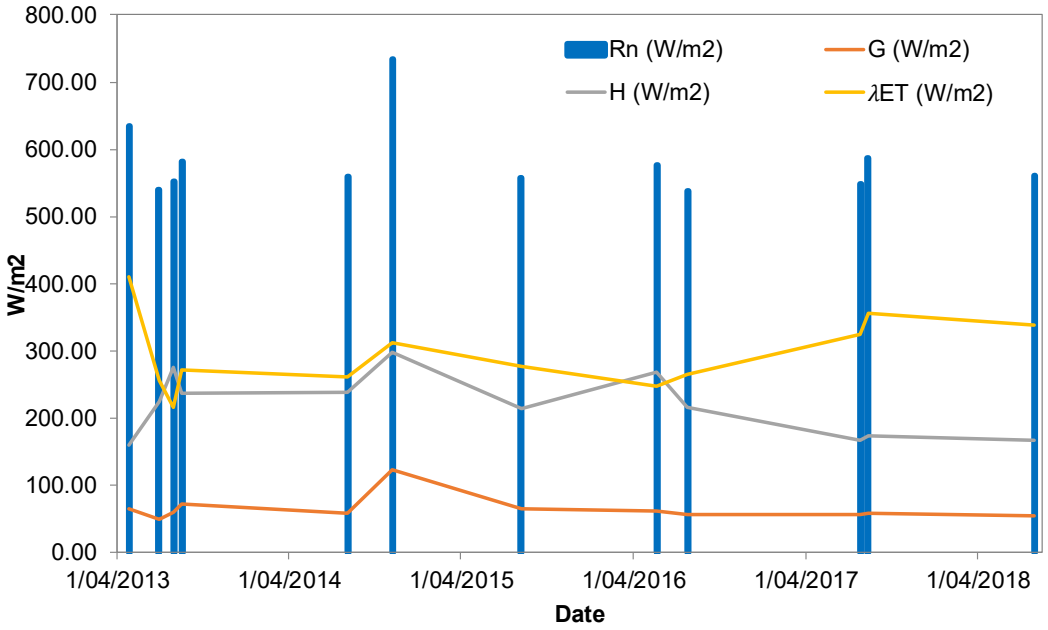

Figure 3: Estimated values of Rn, G, H y λET for 2013 to 2018.

Soil heat flux (G)

To make its estimation the main input parameters are the surface temperature, the NDVI, the surface albedo and the net radiation. Figure 3 shows that for the analysis dates the results oscillate between [10.31 - 155.32] W/m2, higher values at 129.13 W/m2 they are on bare soil and/or sparsely vegetated, and in vegetated agricultural areas they present lower values ranging between [49.81 - 129.13] W/m2.

Sensible heat flux (H)

For the dates of analysis, the results oscillate between [-175.65 - 1337.75] W/m2. Values greater than 400.69 W/m2 of H occur in areas without cultivation or with NDVI values close to zero and the lowest values of 85.80 to 400.69 W/m2 occur in areas with vegetation. In areas with very high slopes, or high temperatures above normal ranges, due to sensor inaccuracies, there are negative values out of range, the SEBAL model performs well in areas with flat slopes, the values are acceptable approximations[28].

Latent heat flux (λET)

The results range between [-1274.91 - 995.48 W/m2]. The areas with vegetation represent high values of 128.39 to 480.83 W/m2 and in areas without crops they present values very close to zero. In areas with very high slopes, or high temperatures, there are negative values greater than 480.83 W/m2 that are out of range, while in areas with flat slopes the values are acceptable. Latent heat flux fluctuations do not behave well in areas with very high slopes[29].

3.2 Daily actual evapotranspiration (ET24)

Table 3 shows the minimum, average and maximum values for the analysis dates. Values less than 1.50 mm/day correspond to areas with soils without cultivation or soils with low vegetation cover (NDVI <0.21) and, on the other hand, areas covered with vegetation or grasslands (NDVI> 0.41) represent values between 1.50 at 4.20 mm/day. Negative values greater than 4.20 mm/day of evapotranspiration correspond to mountain areas with steep slopes. For practical purposes negative values are considered zero. In general, these evapotranspiration rates are high values compared to the annual precipitation in the Lake Titicaca basin[30], which can have detrimental effects on agriculture in the region.

Table 2. Statistical values of daily real evapotranspiration (ET24), SEBAL methodology

Image Dates	ET24 (mm/day)		
	Minimum	Average	Maximum
26/04/2013	-3.7	2.2	3.8
29/06/2013	-16.7	1.6	4.1
31/07/2013	-12.2	1.8	8.5
16/08/2013	-8.0	3	8
03/08/2014	-9.3	2.5	7.3
07/11/2014	-11.9	3.6	7.4
06/08/2015	-7.1	3	8.2
20/05/2016	-17.2	2.8	6.9
23/07/2016	-10.8	2.5	6
26/07/2017	-13.0	2.2	4.2
11/08/2017	-9.6	2.7	6.1
29/07/2018	-10.3	2.3	4.8

3.3 Estimation of the ETR using the evaporimeter pan method

Huancané Station

Table 3 shows actual evapotranspiration (ETR) results for the Huancané meteorological station. For the natural pasture zone, the values vary from 1.56 to 3.51 mm/day with an average of 2.10 mm/day and cultivated pastures range between [1.91 - 3.90] mm/day with an average of 2.44 mm/day.

Muñani Station

Table 4 shows actual evapotranspiration results (ETR) using climatic data from the Muñani station. For the area of natural pastures, with values that vary between [1.36 - 2.50] mm/day with an average of 1.76 mm/day and cultivated grasses range between [1.66 - 2.80] mm/day with an average of 2.04 mm/day.

Comparison and validation of evapotranspiration results

The ETa estimates of the SEBAL model were validated with the values obtained from the evaporimeter pan. A broad overview of the calculated basin-level latent heat flux and evapotranspiration values is shown in Figure 4a and Figure 4b respectively.

Table 3. Actual evapotranspiration values, evaporimeter pan method, Huancane station

Image Dates	ETo (mm/día)	Natural pastures		Cultivated pastures	
		Crop coefficient Kc	ETR (mm/día)	Crop coefficient Kc	ETR (mm/día)
26/04/2013	2.18	0.9	1.96	0.99	2.15
29/06/2013	2.10	0.9	1.89	0.98	2.06
31/07/2013	2.48	0.63	1.56	0.77	1.91
16/08/2013	2.78	0.71	1.97	0.83	2.30
03/08/2014	2.33	0.71	1.65	0.83	1.93
07/11/2014	3.90	0.9	3.51	1.00	3.90
06/08/2015	3.12	0.71	2.22	0.83	2.59
20/05/2016	3.45	0.9	3.11	1.01	3.48
23/07/2016	3.23	0.63	2.03	0.77	2.48
26/07/2017	2.63	0.63	1.65	0.77	2.02
11/08/2017	3.00	0.71	2.13	0.83	2.49
29/07/2018	2.48	0.63	1.56	0.77	1.91
		Minimum	1.56		1.91
		Maximum	3.51		3.90
		Average	2.10		2.44

Table 4. Actual evapotranspiration values, using the evaporimeter pan method, Muñani station

Image Dates	ETo (mm/día)	Natural pastures		Cultivated pastures	
		Crop coefficient Kc	ETR (mm/día)	Crop coefficient Kc	ETR (mm/día)
26/04/2013	2.10	0.9	1.89	0.99	2.08
29/06/2013	1.80	0.9	1.62	0.98	1.76
31/07/2013	2.25	0.63	1.42	0.77	1.73
16/08/2013	2.10	0.71	1.49	0.83	1.74
03/08/2014	2.25	0.71	1.60	0.83	1.87
07/11/2014	2.18	0.9	1.96	1.00	2.18
06/08/2015	2.40	0.71	1.70	0.83	1.99
20/05/2016	2.78	0.9	2.50	1.01	2.80
23/07/2016	3.04	0.63	1.92	0.77	2.34
26/07/2017	2.48	0.63	1.56	0.77	1.91
11/08/2017	2.93	0.71	2.08	0.83	2.43
29/07/2018	2.16	0.63	1.36	0.77	1.66
		Minimum	1.36		1.66
		Maximum	2.50		2.80
		Average	1.76		2.04

An acceptable relationship was found between the ETR SEBAL method and the evaporimeter pan method during the 2013 and 2018 seasons with a coefficient of determination (R^2) of 0.93 (Figure 5). The mean square error (RMSE) was 0.14 mm/day. The Nash-Sutclife efficiency was 0.82, this value being good[31]. The average daily ETR was 2.44 mm/day.

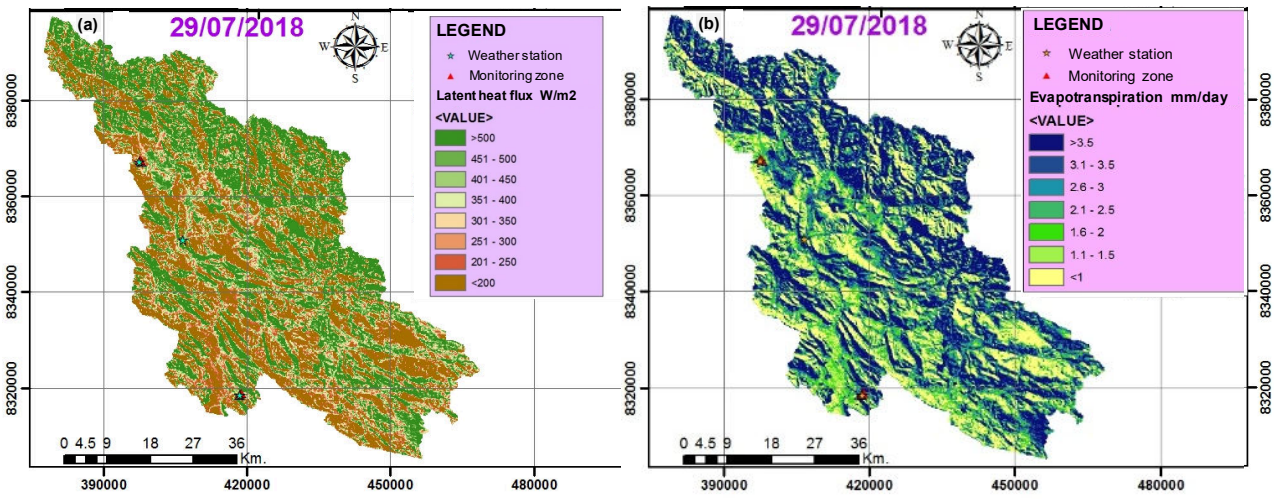

Figure 4: Results for July 29, 2018 a) Latent heat flux b) Evapotranspiration in the basin.

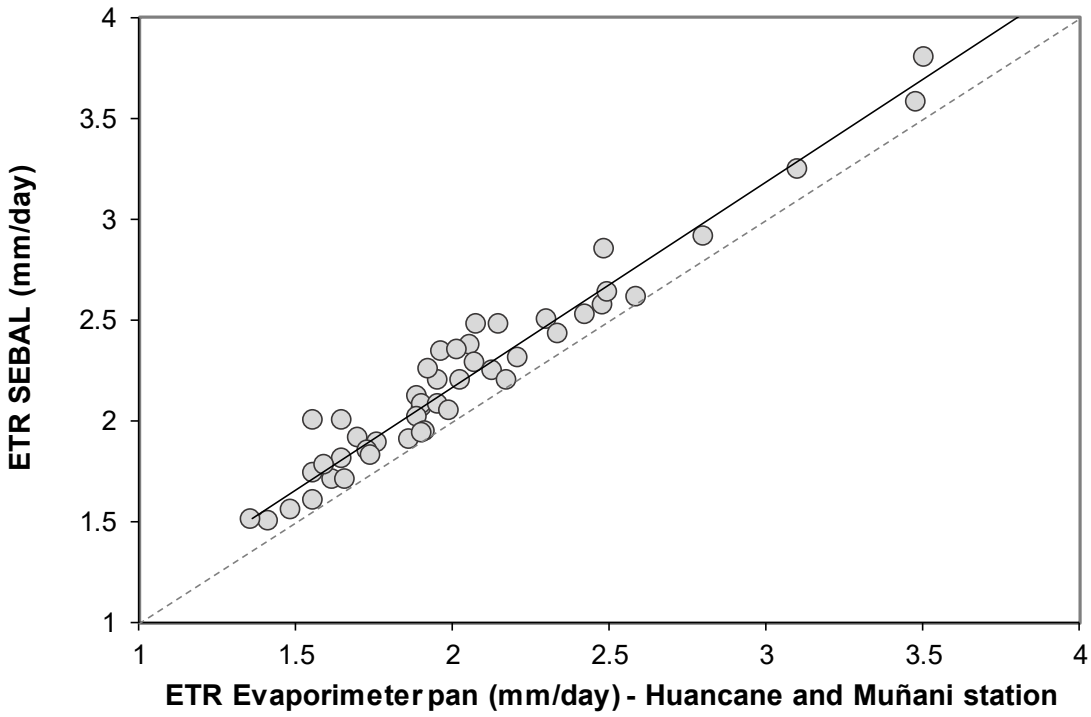

Figure 5: Relationship between ETR estimate by SEBAL and evaporimeter pan

4. CONCLUSION

In the Huancané basin, evapotranspiration was estimated using the SEBAL model, based on images from the Landsat 8 satellite. According to the results, the model behaves well for the flat areas of the basin, which shows that it is feasible to use the model to perform reliable estimates of evapotranspiration. However, in mountain areas with steep slopes, results were obtained with negative values outside the acceptable range.

In addition, it can be concluded that the SEBAL model provided satisfactory results compared to the evaporimeter pan measurements. In this study, the SEBAL method had an acceptable performance for ETR estimates during the period analyzed. This indicates that the method can be used to estimate crop water needs on a regional and field scale in regions where the required data exist and where greater uncertainty is acceptable. The results provided a better understanding of evapotranspiration according to the most frequent natural and cultivated pasture covers and energetic conditions in the Peruvian Altiplano basins.

REFERENCES

[1] Li, Z., Liu, X., Ma, T., Kejia, D., Zhou, Q., Yao, B. and Niu, T., "Retrieval of the surface evapotranspiration patterns in the alpine grassland-wetland ecosystem applying SEBAL model in the source region of the Yellow River, China," Ecol. Modell. **270**, 64–75 (2013).

[2] Liu, S. M., Xu, Z. W., Zhu, Z. L., Jia, Z. Z. and Zhu, M. J., "Measurements of evapotranspiration from eddy-covariance systems and large aperture scintillometers in the Hai River Basin, China," J. Hydrol. **487**, 24–38 (2013).

[3] Dong, W., Li, C., Hu, Q., Pan, F., Bhandari, J. and Sun, Z., "Potential Evapotranspiration Reduction and Its Influence on Crop Yield in the North China Plain in 1961–2014," Adv. Meteorol. **2020**, S. Tariq, Ed., 3691421 (2020).

[4] Gordillo Salinas, V. M., Flores Magdaleno, H., Tijerina Chávez, L. and Arteaga Ramírez, R., "Estimación de la evapotranspiración utilizando un balance de energía e imágenes satelitales," Rev. Mex. ciencias agrícolas **5**(1), 143–155 (2014).

[5] Nassery, H. R., Adinehvand, R., Salavitabar, A. and Barati, R., "Water management using system dynamics modeling in semi-arid regions," Civ. Eng. J. **3**(9), 766–778 (2017).

[6] Pilares-Hualpa, I., Alfaro-Alejo, R., Pilares-Hualpa, R. and Pilares-Calla, C., "Application of an optimization model for the water management under climate scenarios of the Lagunillas integral system of the peruvian Altiplano," 38th IAHR World Congr., 5847–5856, IAHR, Panama (2019).

[7] Reyes-González, A., Kjaersgaard, J., Trooien, T., Hay, C. and Ahiablame, L., "Estimation of Crop Evapotranspiration Using Satellite Remote Sensing-Based Vegetation Index," Adv. Meteorol. **2018**, J. Friesen, Ed., 4525021 (2018).

[8] Thakur, J. K., Singh, S. K. and Ekanthalu, V. S., "Integrating remote sensing, geographic information systems and global positioning system techniques with hydrological modeling," Appl. Water Sci. **7**(4), 1595–1608 (2017).

[9] Bastiaanssen, R., "Regionalization of surface flux densities and moisture indicators in composite terrain A remote sensing approach under clear skies in mediterranean climates" (1995).

[10] Taipe, C. L. R. and Ticona, U. C., "Evapotranspiration modelling in the high Andeans zones of Peru using remote sensing techniques," 38th IAHR World Congr., Panama (2019).

[11] Grosso, C., Manoli, G., Martello, M., Chemin, Y. H., Pons, D. H., Teatini, P., Piccoli, I. and Morari, F., "Mapping Maize Evapotranspiration at Field Scale Using SEBAL: A Comparison with the FAO Method and Soil-Plant Model Simulations," Remote Sens. **10**(9) (2018).

[12] Vicente Liendro Moncada, J., José Araújo da Silva, T., José, J. V., Bonfim-Silva, E. M., Fenner, W. and Oliveira, N. P. R. de., "Evapotranspiration mapping of cotton fields in Brazil: comparison between SEBAL and FAO-56 method," Geocarto Int., 1–17 (2021).

[13] Gomide, R. L. and de Paula Boratto, I. M., "Evapotranspiration and energy balance components spatial distribution in the north region of Minas Gerais, Brazil, using the SEBAL model and Landsat 5 TM images," Remote Sens. Agric. Ecosyst. Hydrol. XVI **9239**, 92390K, International Society for Optics and Photonics (2014).

[14] Zamani, S. and Rahimzadegan, M., "Mapping dam lake evaporation using SEBAL evapotranspiration model

Case study: Amir Kabir Dam," Sci. Res. Q. Geogr. Data **27**(106), 57–69 (2018).
[15] ALA/Huancané., [Estudio Hidrológico de las Cuencas Huancané y Suches] (2010).
[16] Mohan, M. M. P., Kanchirapuzha, R. and Varma, M. R. R., "Review of approaches for the estimation of sensible heat flux in remote sensing-based evapotranspiration models," J. Appl. Remote Sens. **14**(4), 1–31 (2020).
[17] Li, H., Chen, Z., Jiang, Z., Sun, L., Liu, K. and Liu, B., "Temporal-spatial variation of evapotranspiration in the Yellow River Delta based on an integrated remote sensing model," J. Appl. Remote Sens. **9**(1), 96047 (2015).
[18] Zeng, L., Song, K., Zhang, B., Li, L. and Wang, Z., "Evapotranspiration estimation using moderate resolution imaging spectroradiometer products through a surface energy balance algorithm for land model in Songnen Plain, China," J. Appl. Remote Sens. **5**(1), 1–15 (2011).
[19] Allen, R. G. and Pereira, L. S., [Evapotranspiración del cultivo: Guía para la determinación del requerimiento de agua del cultivo. FAO :Estudios FAO Riego y Drenaje 56, 297.] (2006).
[20] Gordillo, V., "Estimación de la evapotranspiración de un cultivo de vid con apoyo de imagen satelital y validación utilizando Eddy Covariance." (2013).
[21] Nelli, N. R., Temimi, M., Fonseca, R. M., Weston, M. J., Thota, M. S., Valappil, V. K., Branch, O., Wizemann, H.-D., Wulfmeyer, V. and Wehbe, Y., "Micrometeorological measurements in an arid environment: Diurnal characteristics and surface energy balance closure," Atmos. Res. **234**, 104745 (2020).
[22] Branch, O., Warrach-Sagi, K., Wulfmeyer, V. and Cohen, S., "Simulation of semi-arid biomass plantations and irrigation using the WRF-NOAH model – a comparison with observations from Israel," Hydrol. Earth Syst. Sci. **18**(5), 1761–1783 (2014).
[23] Júnior, J. B. C., Lucena, R. L., da Silva, H. J. F., dos Reis, J. S. and Rodrigues, D. T., "Considerações sobre a evapotranspiração estimada pelo algorítimo SEBAL no semiárido brasileiro," Rev. Geociências do Nord. **7**(1), 45–51 (2021).
[24] Sahnoun, F., Abderrahmane, H., Kaddour, M., Abdelkader, K., Mohamed, B. and Castro, T. A. H. de., "Aplicação de SEBAL e Ts/VI Trapézio Modelos para Estimar a Evapotranspiração Real no Ambiente do Argelino Semi-árido para Melhorar a Gestão da água na Agricultura," Rev. Bras. Meteorol.(ahead) (2021).
[25] British, N., Waters, R., Allen, R., Tasumi, M., Trezza, R. and Bastiaanssen, W., "SEBAL, Surface Energy Balance Algorithms for Land. Advance Training and Users Manual. Idaho: a NASA EOSDIS/Synergy grant from the Raytheon Company University of Idaho.," 1–97 (2002).
[26] Huamán, H., "Estimación espacial de la Evapotranspiración real usando imágenes de satélite mediante el algoritmo SEBAL caso: Irrigación Majes I- Arequipa." (2015).
[27] Gamboa, W. and Moreno, E., "Cálculo de evapotranspiración para la subzona hidrográfica río Tapias y otros directos al Cauca en el departamento de Caldas, Colombia." (2019).
[28] He, J., Zhao, W., Li, A., Wen, F. and Yu, D., "The impact of the terrain effect on land surface temperature variation based on Landsat-8 observations in mountainous areas," Int. J. Remote Sens. **40**(5–6), 1808–1827 (2019).
[29] Nuñez Julía, C. M., "Modelación del flujo de calor del suelo y aplicación de algoritmo de cálculo de evapotranspiración mediante teledetección." (2009).
[30] Laqui, W., Zubieta, R., Rau, P., Mejía, A., Lavado, W. and Ingol, E., "Can artificial neural networks estimate potential evapotranspiration in Peruvian highlands?," Model. Earth Syst. Environ. **5**(4), 1911–1924 (2019).
[31] Ritter, A. and Muñoz, R., "Performance evaluation of hydrological models: Statistical significance for reducing subjectivity in goodness-of-fit assessments," J. Hydrol. **480**, 33–45 (2013).